Raman spectra and DFT calculations of thiophenol molecules adsorbed on a gold surface

A. Merlen, Dorothée Berthomieu, Mathieu E Edely, Michel Rérat

RAMAN SPECTRA DFT CALCULATIONS OF THIOPHENOL MOLECULES ADSORBED ON A GOLD SURFACE

A. Merlen[1*], D. Berthomieu[2], M. Edely[3], M. Rerat[4]

1 IM2NP, Univ Toulon and Aix-Marseille Univ, CNRS, UMR 7334, site de Toulon, France

2 ICGM, Université Montpellier, CNRS, ENSCM, Montpellier, France

3 Institut des Molécules et Matériaux du Mans, Le Mans Université, CNRS, UMR 6283, France

4 Université de Pau et des pays de l'Adour, CNRS, IPREM UMR 5254, E2S UPPA, Pau, France

Keywords : DFT, SERS, Thiophenol, Gold

* merlen@univ-tln.fr, present address: MAPIEM (Matériaux Polymères Interfaces Environnement Marin) , University of Toulon, France

Abstract

We report the calculation of Raman modes of thiophenol molecules adsorbed on a real gold surface. The calculated Raman spectra strongly depend on the absorption configuration of the molecule on the metallic surface, a feature that should be carefully taken into account in the interpretation of Surface Enhanced Raman Spectra (SERS). The calculated Raman spectra are compared with experimental SERS measurements, best accordance being obtained for a tilted configuration of the absorbed molecule. The present study supports the necessary combination of computational approaches with SERS measurements to predict the type of molecular adsorption configurations on metallic surfaces.

Introduction

Since its discovery at the end of the 70's, SERS is considered as an extremely promising analytical method for the detection of low concentration chemical species. Its application covers a very broad field: detection of drugs or illegal substances[1], analysis of pollutant molecules in water[2–4], identification of chemical species at the surface of metals[5], study of pigments in art or archeology[6,7], and many others.

Its basic principle is now well known[8]: it is based on the giant electromagnetic field enhancement in the optical near field of plasmonic nanoparticles (usually gold or silver)

leading to a huge increase of the Raman cross section[9]. This mechanism is called the Electromagnetic Enhancement (EM) in SERS. The relation between the efficiency of the optical nano-antenna and the final enhancement of the Raman scattering is now clearly established[10].

Compared to classical Raman spectroscopy, the sensitivity of SERS is so high that single molecule detection (SMD) has been reported[11–13]. Nevertheless, SMD requires the combination of many features, in particular the resonant process, and is thus practically limited to a small number of molecules, mainly dye molecules such as Rhodamine 6G. Anyway, SERS has proven its efficiency for the detection of molecules at very low concentrations and hopefully SMD sensitivity is not required for most applications.

For the identification of chemical species with SERS, the protocol is usually the following: the recorded SER spectrum is compared with a database of SERS spectra. This is a first limitation, as the SER spectra of most chemical species remain unknown. To avoid this problem, standard Raman spectra databases are used. This method is extremely uncertain, as the SERS spectrum of a chemical species can be very different compared to its normal one: some modes are shifted, new peaks are observed and the intensity of every mode may vary, strongly. Therefore misidentifications may be done. This is unacceptable for the use of SERS as an analytical tool. It is thus necessary to have a clear understanding of the origin of those changes in the SERS signature of a given molecule. Many hypothesis were advanced to explain differences between the SER and normal Raman spectra. For several molecules, SER may result from a chemical reaction activated via a plasmonic mechanism. This is the case for instance with aminothiophenol or nitrothiophenol[14]. For those molecules the new Raman modes originate from the chemical species formed during the laser activated chemical reaction[15]. DFT calculations have proven that those modes are coming from azo compounds resulting from the reaction between nitro or amino groups[16]. Fortunately this situation is unusual and limited to a low number of molecules[17]. Therefore, most of the changes observed in SERS spectra in comparison with Raman spectra originate from intrinsic molecular properties.

To explain those changes a first simple hypothesis is a mere deformation of the molecule during the adsorption process. Specific chemical bonds between the molecule and the metallic atoms can be formed. The molecule itself may change its shape due to the interaction with the surface. Both processes will lead to changes in the Raman signature of the molecule. Therefore it is essential to have a clear idea of the adsorption process.

A second hypothesis can be advanced: the changes in the SER spectra have sometimes been considered as an experimental proof of the so-called Chemical Enhancement (CE) mechanism of SERS. CE and EM act together during the enhancement process[18,19]. Even if suggested very early in the understanding of SERS, CE has been the object of strong debates for several decades and remains largely unclear. It is now admitted that it is based on a charge transfer mechanism between the molecule and the metallic surface[20]. An important point is to determine if this charge transfer is required to explain the spectral changes observed in SERS.

To answer those important questions we propose to compare the calculated Raman spectra of the thiophenol molecule (also known as benzenethiol or phenylmercaptan) interacting with a crystalline gold surface. This molecule offers several advantages for SERS. First, it has a thiol functional group that has a strong affinity for metallic surfaces. Its adsorption mechanism, via both physisorption and chemisorption processes[21], is well known (release of an hydrogen atom) and the SERS measurements are easy. Tip Enhanced Raman Spectroscopy (TERS) measurements have been reported with this molecule, even if TERS is a very demanding technique[22]. Secondly, its SER spectrum is significantly different from its normal one. Those differences have been reported in previous publications[23,24] but no clear explanations have been proposed so far. A previous studies has suggested that depolarization, orientation of the adsorbate and surface roughness could play a role[25], but no experimental nor numerical proof have been proposed to confirm those hypothesis. This question is important as thiophenol-based molecules offer the possibility to amplify the sensitivity and improve the chemical selectivity of functionalized SERS surfaces[26].

Our results demonstrate that the orientation of the molecule on the metallic surface strongly influences the calculated Raman spectra. We suggest that the comparison between calculated and measured spectra gives information about the density and the orientation of adsorbed molecules on the gold surface. A detailed interpretation of the SERS spectrum can bring information far beyond the simple identification of chemical species.

Methods

The number of numerical methods developed for the calculation of SER spectra is extremely large. The complete theory of SERS, still under debate, is complex and requires taking into

account many features: charge transfer, adsorption mechanism, quantum features, resonance[27], specific intramolecular interactions in Self Assembled Monolayers…..Up to now there is no numerical method taking into account all those parameters. Morton and Jensen have proposed in 2009[28] a quantum mechanical approach to model the interaction between a single pyridine molecule and a small silver cluster for a better understanding of the chemical enhancement providing the SERS enhancement. Their approach was based on a single adsorbed molecule avoiding any interaction of molecules between each other and thus did not consider the intramolecular interaction that should be taken into account for the interpretation of standard SERS measurements. In addition, due to its limited size, the metallic cluster is far to mimic real metallic surfaces[29]. To address this important question, we focused our study on standard DFT calculations with a large metallic surface. We deliberately choose a simple method giving a good compromise between efficiency, simplicity and calculation costs. DFT calculation of the periodic system were performed with the Crystal Software[30–31]. We used a GGA PW91 Hamiltonian[32] since it is known to be very efficient for the calculations of thiophenol molecules on gold[33]. Standard basis set for gold[34], carbon[35], hydrogen[35] and sulfur[36] atomic orbitals which can be found on the Crystal Website[37] were considered. First, a Self-Consistent Field (SCF) calculation is done in order to obtain the unperturbed energy and electron density at the optimized geometry, then the Coupled-Perturbed Hartree-Fock and Kohn-Sham (CPHF/CPKS) method implemented in Crystal is used to calculate the infrared and Raman intensities[38–41] after having obtained the vibrational frequencies[42-43].

Computed SER spectrum reported in the literature are frequently using only few atoms of the metal support to simulate the whole metallic surfaces[44,45]. This is a huge approximation and we believe that it is not acceptable for the calculation of a real SER spectrum, a point that has already been evocated by Holze[46]. We have thus chosen to calculate the Raman spectrum of thiophenol in interaction with a crystalline (111) gold surface made of two layers of metallic atoms. Different densities of adsorbed molecules were consider. The 2D periodicity of the complete system (molecule+metallic surface) depends on this density. For each configuration, only one molecule is present in the periodic cell.

For the calculations of vibrational modes, only the atoms of the thiophenol molecule have been set free. Gold atoms are fixed and modes from the metallic surface are thus not calculated.

We have not taken into account any polarization features for the calculation of the Raman spectra. No scaling factor was applied to frequency values of SER spectra, suggesting that present choices of basis sets and method offer a good agreement with experimental results.

Experimental SER spectrum of thiophenol has been recorded using gold nanocylinders (190 nm diameter) as nano-antenna and a 785 nm laser excitation. The concentration of the thiophenol solution was 10^{-2} mol/L. To avoid any multi-layer configuration we also performed measurements with lower concentrations (down to 10^{-6} mol/L) but the spectrum was not affected except a lower signal to noise ratio.

Results and discussion

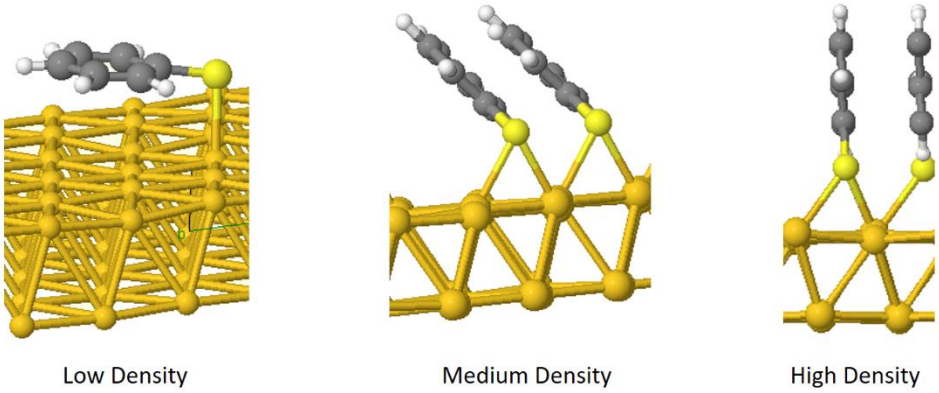

Figure 1: The optimized geometry for the three different absorption configurations.

Before calculating the Raman spectrum, we have first optimized the geometry of our system. Three configurations have been considered: a Low Density (LD) of adsorbed molecules, a Medium density (MD) and a High Density (HD). The final optimized geometry for each configuration is shown in figure 1.

For the low-density configuration, the aromatic ring is lying parallel to the metallic surface. This result is in accordance with Tandiana et al.[47], who indicated that benzene preferred to adopt a flat configuration on gold nanoparticles. In contrast, when the density is high, the steric hindrance would induce a strongly different orientation of benzene so that the molecule is now oriented vertically to the surface. This result suggested that the key role of intramolecular forces, in opposition with what was reported for a single molecule interacting with nanoclusters. For medium density, the position of the molecule would be intermediate and the molecule is tilted, with a tilt angle of ≈110°, which is higher than what was estimated by Carron et al. using SERS (76°)[48]. Nevertheless those configurations are in good agreement

with previous numerical studies[33,49]. It must be noticed that, whatever the configuration, the shape of the molecules remains the same during the adsorption process. We calculated slight changes in the length of chemical bonds. For instance the length of C-C bonds in the benzene ring of the thiophenol was calculated to be 1.4, 1.42, 1.41 Å for the high, low and medium density, respectively, whereas it was calculated to be 1.41 Å for the free benzene ring of the thiophenol.

Now that the geometry is optimized, vibrational modes and Raman spectra have been calculated. Using GGA DFT calculations Tandiana et al.[50] have recently demonstrated that the IR spectrum of aromatic compounds in interaction with a gold nanoparticle was changed as a result from the molecular orientation: they have considered the "flat" and "perpendicular" configurations. Here we have calculated the Raman spectra for the different orientation shown in Figure 1. Obtained spectra are shown in Figure 2, in comparison with the calculated spectrum from the single molecule. Surprisingly those spectra are all very different! New

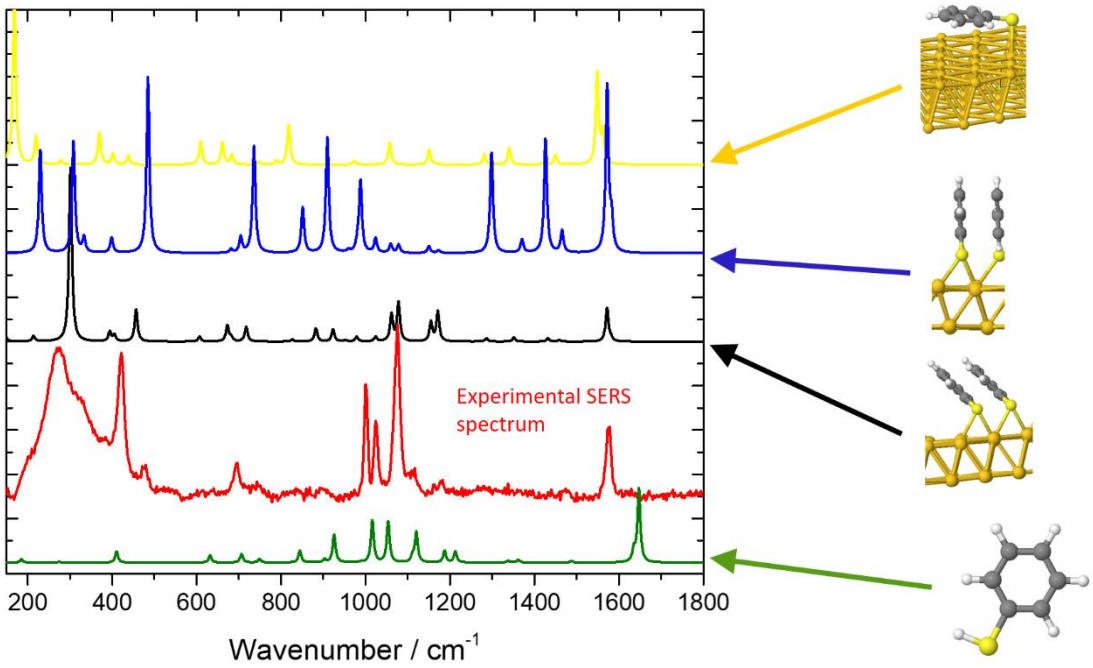

Figure 2: Calculated Raman spectra for the three different adsorption configurations and for the free molecule. The experimental SERS spectrum is also reported.

modes have appeared, some others are strongly shifted and strong variations in intensity are also observed. This result demonstrates that the adsorption configuration of the molecule, in particular its orientation towards the metallic surface, strongly affects the calculated Raman spectra.

To have a better understanding of the origin of those changes, we will now focus our attention on two specific spectral regions: the low wavenumber region, between 150 and 500 cm^{-1} and the middle wavenumber region, between 900 and 1200 cm^{-1}.

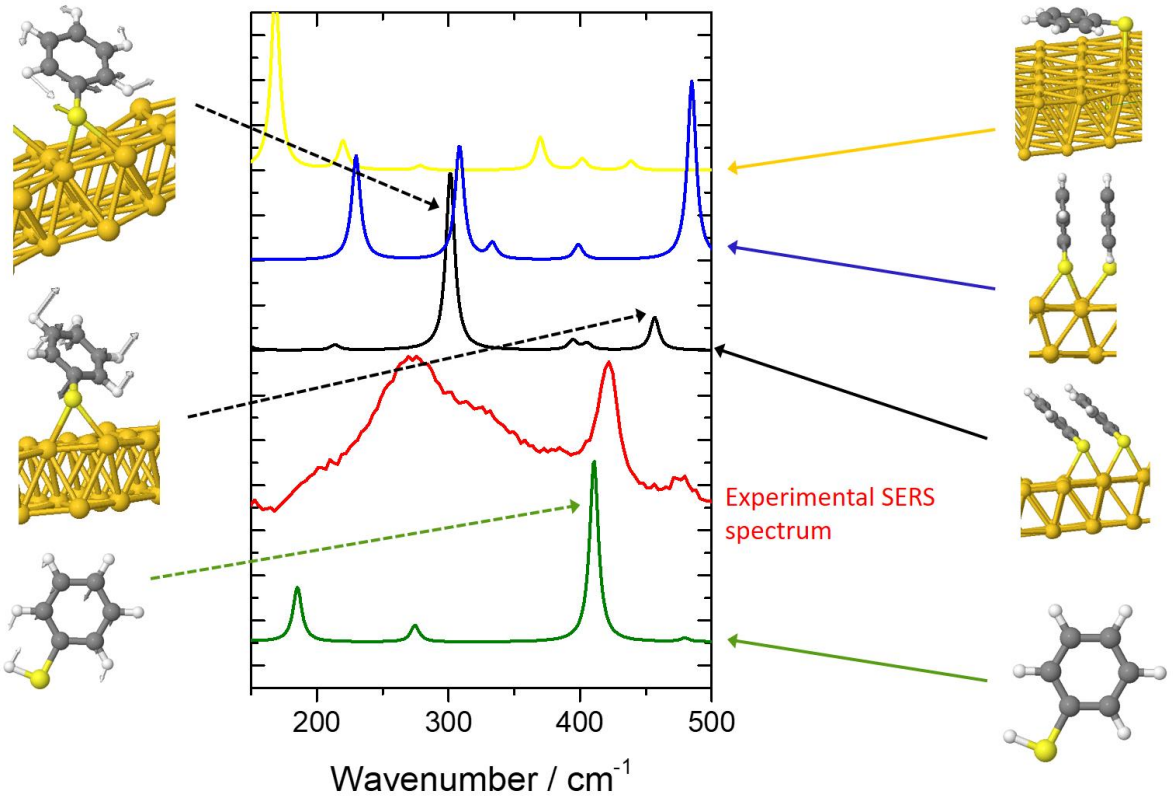

Figure 3: Calculated and measured Raman spectra in the low wavenumber region. Some specific vibrational modes are also shown.

The measured and calculated SER spectra in the low wavenumber region are shown in Figure 3. In the experimental SER spectrum two main contributions are observed: a broad and very intense mode centered around 270 cm^{-1} and a sharper mode at 420 cm^{-1}. This spectral region is important in SERS as it contains the vibrational signature of the molecule-surface interaction: some modes are related to the S-Au bond[46]. This is the case for the broad 270 cm^{-1} mode[48]: it is absent (or very weak) for the molecule alone but related modes close to this wavenumber are systematically observed when the molecule is linked via an S-Au bond to the

gold surface. Those modes can be reasonably associated to the spectral signature of the S-Au bond formed during the adsorption of the molecule on the gold surface. This hypothesis is confirmed if we look carefully at the nature of the intense 300 cm^{-1} mode calculated for the medium density. As can be seen in the left part of figure 3, this mode is directly related to the S-Au bond. Nevertheless it cannot be attributed to a single Au-S stretching[46] or bending vibration[44] or a pure ring mode. Our calculations demonstrate that it is rather a combination of both contributions. We would like to emphasize the fact that the interpretation of low frequency modes is not straightforward and most of the calculated modes in this spectral region are a complex combination of vibrations involving the whole molecule and its bond with the metallic surface. In opposition, the mode at 420 cm^{-1} is not specific to the interaction with the surface as it is clearly present when the molecule is alone. This mode corresponds to a combination of in-plane and out-of-plane vibrations of the aromatic ring. Using silver SERS susbtrates, Aggarwal et al.[24] have observed an upshift of 6 cm^{-1} between the standard and the SERS spectrum for this mode. In our calculation, it is shifted and gives rise to several peaks with various wavenumbers and intensity depending on the molecular orientation. A single and significantly upshifted peak is observed for the HD configuration, whereas for the MD a doublet is formed. For the LD multiple and strongly downshifted peaks are present. It appears in the experimental SERS spectrum, and is confirmed in other SERS studies[23], that a doublet is observed at 420 and 475 cm^{-1}, this last peak having a much lower intensity. This doublet is the signature of the interaction of the molecule with the metallic surface leading to a removal of degeneracy. The best agreement in wavenumber between the experimental and calculated Raman spectra is obtained for the medium density, that is to say when the molecule is tilted towards the surface. We can reasonably assume that the observed peaks at around 450 cm^{-1} correspond to the out of plane mode shown in Figure 3. This suggests that, in opposition to what is proposed by Holze et al.[46], out of plane modes can be observed by SERS. We believe that the determination of molecule orientation by simple geometry consideration (observation of out-of or in-plane vibrations) might be tricky.

Let's move now towards the intermediate wavenumber region, shown in Figure 4. This region is crucial, as it is there that the observed differences between standard Raman and SERS spectra are the most important. The main difference is the giant enhancement of modes at around 1080 cm^{-1}, very weak in the standard Raman spectrum of the molecule but very

intense in SERS. The tilted and the flat configuration give rise to intense calculated modes at this wavenumber. It is not the case with the molecule standing vertically, obviously this configuration does not correspond to the experimentally measured SER spectrum. As a consequence we can reasonably assume that, combining the analysis of both low and medium wavenumber regions the best agreement between measured and calculated SERS spectra is obtained for the medium density configuration, that is to say when the molecule is tilted.

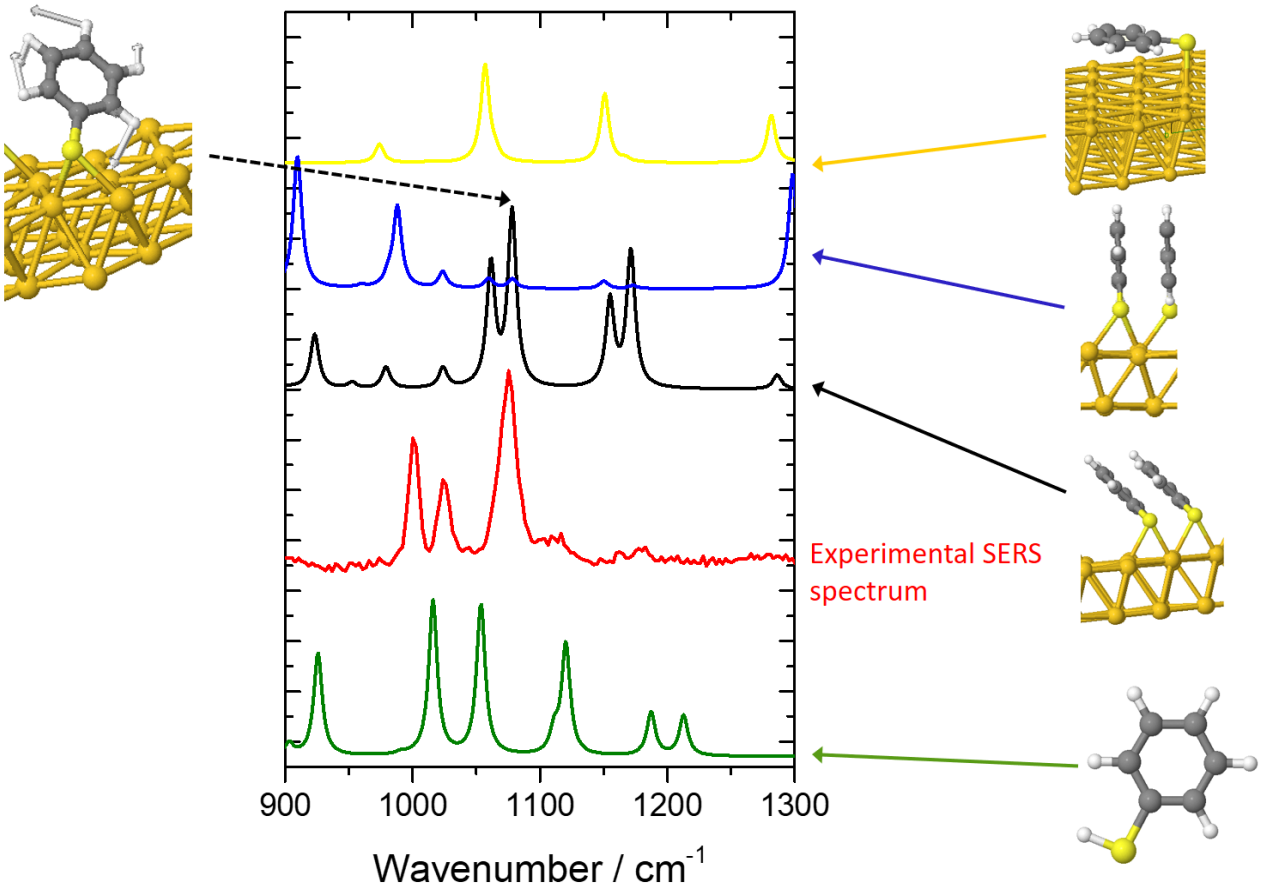

Figure 4: Calculated and measured Raman spectra in the intermediate wavenumber region.

This result corresponds to what is generally concluded for the adsorption on gold of this molecule. We will not consider the 1600 cm^{-1} region as it is sensitive to photoinduced charge transfer processes[51], a feature that we have deliberately not taken into account in our approach.

Clearly, the agreement between calculated and measured Raman spectra is not perfect, some differences remain. A first important difference is the broad and intense mode at 270 cm^{-1}.

We have suggested that this mode is related to the S-Au bond, a reasonable hypothesis confirmed by Nyamekye et al.[25] using directional Raman scattering. To be so broad this peak is probably a combination of various vibrational modes, each one being associated to a specific S-Au bond. In our calculations, we have assumed a perfect and crystalline gold surface which is not the case with real gold nanoparticles. There is probably a wide range of various adsorption sites, each one giving a characteristic vibrational signature. Their combinations gives rise to the broad and intense S-Au peak. This feature explains the difference between calculated and measured Raman spectra at 270 cm^{-1}. There are other differences, in particular in the intermediate frequency region. For the tilted molecules, which we assumed as the preferred configuration, calculated Raman modes are supposed to occur at 1170 cm^{-1} (a doublet), they are indeed observed in the SERS spectrum but with a very low intensity compared to the other modes. It appears almost impossible to have a perfect match between measured and calculated Raman spectra. Once again, those differences are probably coming from the fact that we consider a clean gold surface and a perfect crystalline adsorption configuration for the thiophenol molecule. Such configuration can be reached with high vacuum deposition devices, with crystalline metallic surfaces. It is impossible with molecules deposited in solution on low crystallinity gold nanocylinders used for SERS measurements. As mentioned by Holze[46], the highly organized arrangements usually assumed for thiol molecules on gold surfaces are not always obtained. In addition, thiophenol is known to form poorly organized SAMs on gold[52]. Our calculations suggest that the dominant configuration corresponds to tilted molecules but many other configurations are also possible. The complex combination of the characteristic vibrational signatures of each one of them leads to the observed SER spectra.

Conclusion

We clearly demonstrated that the orientation of the adsorbed molecule strongly affect its Raman signature, independently from any polarization or change transfer mechanisms. We suggest that the evolution of the SER spectrum itself could be a method to estimate if SMD occurs. For our SERS measurements we have used a relatively high concentration of thiophenol (10^{-2}). We decreased the concentration down to 10^{-8} and did not observe any change in the experimental spectra except a lower signal to noise ratio. For such concentrations, the density of adsorbed molecules is high, and a relatively good agreement is

obtained between measured and calculated Raman spectra for the tilted configuration. Obviously, this does not correspond to SMD. To reach SMD, the density must be decreased towards the low density configuration. In this case, the thiophenol molecule should lie flat on the metallic surface as shown in Figure 1. The SERS spectrum should be thus modified, in agreement with the spectrum calculated for this configuration. We expect severe changes in the low wavenumber region as suggested in Figure 3. Those features do not prove the SMD itself, but they are a necessary condition.

Acknowledgements: This work was performed using HPC resources from GENCI-IDRIS and CINES.

References

1 A. Merlen, C. Pardanaud, K. Gratzer, S. Coussan, D. Machon, A. Forestier, D. Bergé-Lefranc, T. N. T. Phan and V. Hornebecq, *J. Raman Spectrosc.*, 2020, **51**, 2192–2198.

2 O. Péron, E. Rinnert, F. Colas, M. Lehaitre and C. Compère, *Appl. Spectrosc.*, 2010, **64**, 1086–1093.

3 G. Bodelón and I. Pastoriza-Santos, *Front. Chem.*, 2020, **8**, 1–8.

4 J. Hao, M. J. Han, S. Han, X. Meng, T. L. Su and Q. K. Wang, *J. Environ. Sci.*, 2015, **36**, 152–162.

5 A. Merlen, C. Pardanaud, S. Coussan, C. Panagiotopoulos, O. Grauby and C. M. Ruiz, *J. Raman Spectrosc.*, 2018, **49**, 1184–1189.

6 F. Pozzi and M. Leona, *J. Raman Spectrosc.*, 2016, **47**, 67–77.

7 K. L. Wustholz, C. L. Brosseau, F. Casadiob and R. P. Van Duyne, *Phys. Chem. Chem. Phys.*, 2009, **11**, 7348–7349.

8 P. G. Etchegoin and E. C. Le Ru, *Principles of surface-enhanced Raman spectroscopy and related plasmonic effects*, Elsevier, 2009.

9 B. Pettinger, G. Picardi, R. Schuster and G. Ertl, *Single Mol.*, 2002, **3**, 285–294.

10 J. Plathier, A. Merlen, A. Pignolet and A. Ruediger, *J. Raman Spectrosc.*, 2017, **48**, 1–8.

11 K. Kneipp, Y. Wang, H. Kneipp, L. T. Perelman, I. Itzkan, R. R. Dasari and M. S. Feld, *Phys. Rev. Lett.*, 1997, **78**, 1667.

12 E. C. Le Ru and P. G. Etchegoin, *Annu. Rev. Phys. Chem.*, 2012, **63**, 65–87.

13 S. M. Nie, S. R. Emery and S. R. Emory, *Science (80-.).*, 1997, **275**, 1102–1106.

14 A. Merlen, M. Chaigneau and S. Coussan, *Phys. Chem. Chem. Phys.*, 2015, **17**, 19134–19138.

15 Y. F. Huang, H. P. Zhu, G. K. Liu, D. Y. Wu, B. Ren and Z. Q. Tian, *J. Am. Chem. Soc.*, 2010, **132**, 9244–9246.

16 R. Jiang, M. Zhang, S. L. Qian, F. Yan, L. Q. Pei, S. Jin, L. Bin Zhao, D. Y. Wu and Z. Q. Tian, *J. Phys. Chem. C*, 2016, **120**, 16427–16436.

17 C. Zhan, M. Moskovits and Z. Q. Tian, *Matter*, 2020, **3**, 42–56.

18 R. Pilot, R. Signorini, C. Durante, L. Orian, M. Bhamidipati and L. Fabris, *Biosensors*, 2019, **9**, 57.

19 J. Langer, D. J. De Aberasturi, J. Aizpurua, R. A. Alvarez-puebla, B. Auguie, J. J. Baumberg, G. C. Bazan, S. E. J. Bell, A. Boisen, A. G. Brolo, J. Choo, D. Cialla-May, V. Deckert, L. Fabris, K. Faulds, F. J. G. de Abajo, R. Goodacre, D. Graham, A. J. Haes, C. L. Haynes, C. Huck, T. Itoh, M. Käll, J. Kneipp, N. A. Kotov, H. Kuang, E. C. Le Ru, H. K. Lee, J.-F. Li, X. Y. Ling, S. A. Maier, T. Mayerhöfer, M. Moskovits, K. Murakoshi, J.-M. Nam, S. Nie, Y. Ozaki, I. Pastoriza-Santos, J. Perez-Juste, J. Popp, A. Pucci, S. Reich, B. Ren, G. C. Schatz, T. Shegai, S. Schlücker, L.-L. Tay, K. G. Thomas, Z.-Q. Tian, R. P. Van Duyne, T. Vo-Dinh, Y. Wang, K. A. Willets, C. Xu, H. Xu, Y. Xu, Y. S. Yamamoto, B. Zhao and L. M. Liz-Marzán, *ACS Nano*, 2020, **14**, 28–117.

20 L. Xia, M. Chen, X. Zhao, Z. Zhang, J. Xia, H. Xu and M. Sun, *J. Raman Spectrosc.*, 2014, **45**, 533–540.

21 A. Tripathi, E. D. Emmons, S. D. Christesen, A. W. Fountain and J. A. Guicheteau, *J. Phys. Chem. C*, 2013, **117**, 22834–22842.

22 B. Ren, G. Picardi, B. Pettinger, R. Schuster and G. Ertl, *Angew. Chemie - Int. Ed.*, 2004, **44**, 139–142.

23 M. K. Oh, Y. S. Shin, C. L. Lee, R. De, H. Kang, N. E. Yu, B. H. Kim, J. H. Kim and J. K. Yang, *Nanoscale Res. Lett.*, 2015, **10**, 259.

24 R. L. Aggarwal, L. W. Farrar, N. G. Greeneltch, R. P. Van Duyne and D. L. Polla, *Appl. Spectrosc.*, 2012, **66**, 740–743.

25 C. K. A. Nyamekye, S. C. Weibel and E. A. Smith, *J. Raman Spectrosc.*, 2021, **52**, 1246–1255.

26 F. Sun, D. D. Galvan, P. Jain and Q. Yu, *Chem. Commun.*, 2017, **53**, 4550–4561.

27 A. M. Kelley, *J. Chem. Phys.*, 2008, **128**, 224702.

28 S. M. Morton and L. Jensen, *J. Am. Chem. Soc.*, 2009, **131**, 4090–4098.

29 H. Y. Seuret-Hernández, A. Gamboa-Suaréz and C. Morera-Boado, *J. Mol. Graph. Model.*, 2022, **115**, 108234.

30 F. Pascale, C. M. Zicovich-Wilson, F. López Gejo, B. Civalleri, R. Orlando and R. Dovesi, *J. Comput. Chem.*, 2004, **25**, 888–897.

31 C. M. Zicovich-Wilson, F. Pascale, C. Roetti, V. R. Saunders, R. Orlando and R. Dovesi, *J. Comput. Chem.*, 2004, **25**, 1873–1881.

32 R. Dovesi, A. Erba, R. Orlando, C. M. Zicovich-Wilson, B. Civalleri, L. Maschio, M. Rérat, S. Casassa, J. Baima, S. Salustro and B. Kirtman, *Wiley Interdiscip. Rev. Comput. Mol. Sci.*, 2018, **8**, 1–36.

33 R. Dovesi, F. Pascale, B. Civalleri, K. Doll, N. M. Harrison, I. Bush, P. D'Arco, Y. Noel, M. Rera, P. Carbonniere, M. Causa, S. Salustro, V. Lacivita, B. Kirtman, A. M. Ferrari, F. S. Gentile, J. Baima, M. Ferrero, R. Demichelis and M. De La Pierre, *J. Chem. Phys.*, 2020, **152**, 204111.

34 J. P.Perdew and Y. Wang, *Phys. Rev. B*, 1991, **45**, 13244.

35 J. Nara, S. Higai, Y. Morikawa and T. Ohno, *J. Chem. Phys.*, 2004, **120**, 6705–6711.

36 R. Weihrich and I. Anusca, *Zeitschrift fur Anorg. und Allg. Chemie*, 2006, **632**, 335–342.

37 C. Gatti, V. R. Saunders and C. Roetti, *J. Chem. Phys.*, 1994, **101**, 10686–10696.

38 D. Vilela Oliveira, J. Laun, M. F. Peintinger and T. Bredow, *J. Comput. Chem.*, 2019, **40**, 2364–2376.

39 CRYSTAL - Basis Sets Library, https://www.crystal.unito.it/basis-sets.php.

40 L. Maschio, B. Kirtman, R. Orlando and M. Rèrat, *J. Chem. Phys.*, 2012, **137**, 204113.

41 L. Maschio, B. Kirtman, M. Rérat, R. Orlando and R. Dovesi, *J. Chem. Phys.*, 2013, **139**, 2013–2015.

42 L. Maschio, B. Kirtman, M. Rérat, R. Orlando and R. Dovesi, *J. Chem. Phys.*, 2013, **139**, 164101.

43 L. Maschio, B. Kirtman, M. Rérat, R. Orlando and R. Dovesi, *J. Chem. Phys.*, 2013, **139**, 164102.

44 S. Li, D. Wu, X. Xu and R. Gu, *J. Raman Spectrosc.*, 2007, **38**, 1436–1443.

45 H. L. Wu, H. R. Tsai, Y. T. Hung, K. U. Lao, C. W. Liao, P. J. Chung, J. S. Huang, I. C. Chen and M. H. Huang, *Inorg. Chem.*, 2011, **50**, 8106–8111.

46 R. Holze, *Phys. Chem. Chem. Phys.*, 2015, **17**, 21364–21372.

47 R. Tandiana, N. T. Van-Oanh and C. Clavaguéra, *Theor. Chem. Acc.*, 2021, **140**, 1–8.

48 K. T. Carron and L. G. Hurley, *J. Phys. Chem.*, 1991, **95**, 9979–9984.

49 L. F. Peiretti, P. Quaino and F. Tielens, *J. Phys. Chem. C*, 2016, **120**, 25462–25472.

50 R. Tandiana, C. Sicard-Roselli, N.-T. Van-Oanh, S. Steinmann and C. Clavaguéra, *Phys. Chem. Chem. Phys.*, , DOI:10.1039/d2cp02654f.

51 S. P. Centeno, I. López-Tocón, J. Roman-Perez, J. F. Arenas, J. Soto and J. C. Otero, *J. Phys. Chem. C*, 2012, **116**, 23639–23645.

52 E. Sabatani, J. Cohen-Boulakia, M. Bruening and I. Rubinstein, *Langmuir*, 1993, **9**, 2974–2981.